The Effect of Topography on the Dynamics of Interacting Solitary Waves in the Context of Atmospheric Blocking

GEORG GOTTWALD AND ROGER GRIMSHAW

Department of Mathematics and Statistics, Monash University, Clayton, Victoria, Australia

(Manuscript received 20 May 1998, in final form 6 November 1998)

ABSTRACT

It is shown that the influence of topography on the interaction of long, weakly nonlinear, quasigeostrophic baroclinic waves can be described by a pair of linearly coupled Korteweg–de Vries equations, with a forcing term in one of the equations. This system exhibits a rich dynamics that is suggestive of atmospheric blocking such as stable stationary solutions, transient quasi-steady-state solutions, multiple equilibria, and baroclinic instability. Topography is shown to favor the formation of blocking systems. This system is investigated both analytically, using techniques from asymptotic perturbation theory, and through numerical simulations.

1. Introduction

There has been an active research and interest over the past years in atmospheric blocking, that is, the occurrence of quasistationary, highly persistent, coherent structures in the midlatitude lower atmosphere. The understanding of the life cycle of blocking systems is essential for long-range weather forecasting since blocking events may dominate the weather even upstream and downstream of the region where they occur, on a timescale reaching to the lower end of the climatic timescale. The difficulty in formulating a theoretical model for atmospheric blocking is that it involves the interplay of planetary-scale processes, synoptic-scale processes, and orography (see, for instance, Mullen 1987; Lupo and Smith 1995). The analysis of observations suggests that the formation and maintenance can be essentially understood in the framework of quasigeostrophic dynamics (Hansen and Sutera 1984). Quasigeostrophic dynamics can schematically be viewed as a competition between 2D processes and their inherent indirect energy cascade toward large-scale features, and 3D processes and their inherent direct energy cascade toward small-scale features. The former is associated with the Taylor–Proudman theorem, the latter with baroclinic instability, both being features of rotation. There have been two contrasting theoretical approaches. In one, the full quasigeostrophic equations are solved numerically. In the other, reductions of the quasigeostrophic equations are obtained, either in terms of Galerkin approximations (Legras and Ghil 1985) or in terms of a weakly nonlinear analysis and solitary-wave dynamics (Patoine and Warn 1982; Warn and Brasnett 1983; Malguzzi and Malanotte-Rizzoli 1984, 1985; Mitsudera 1994; Helfrich and Pedlosky 1993, 1995; Christensen and Wiin-Nielsen 1996; Gottwald and Grimshaw 1998).

This work is a sequel to our previous work (Gottwald and Grimshaw 1999, hereafter GG) where it was shown that the interaction of long, weakly nonlinear quasigeostrophic waves could be described by a pair of coupled Korteweg–de Vries equations (KdV). This system exhibits a rich variety of dynamics suggestive of atmospheric blocking systems such as stable stationary solutions, transient quasi-stationary solutions, multiple equilibria, and baroclinic instability. We will here continue this work by examining the effect of topography on the formation and development of blocking systems.

Simulations by Lindzen (1986), Kalnay and Mo (1986), Malanotte-Rizzoli and Malguzzi (1987), and Shutts (1983), and observational studies by Shutts (1986) and Illari (1984) suggest that orography is not necessary for the formation and maintenance of a blocking system; but Egger et al. (1986) concede that with only eddy forcing, blocking systems would not have the observed amplitudes when friction is included and, hence, we should take into account the effect of topography. In other words topography is not necessary to obtain blocking systems but does support their development and may be dynamically important. We will address this issue here.

Topography may support large-amplitude, nearly stationary waves through interaction with waves whose phase speed is close to zero in a coordinate frame fixed

Corresponding author address: Dr. Georg Gottwald, INLN-CNRS, 1361 route des Lucioles, 06560 Valbonne Sophia-Antipolis, France. E-mail: gottwald@inln.cnrs.fr.

to the topography. This interaction can occur either through direct resonant forcing or through the trapping of waves traveling toward the topography (e.g., Grimshaw et al. 1995). In both cases the linear phase speed of the waves is close to zero. Both processes make topographic forcing an attractive mechanism for the study of atmospheric blocking. Furthermore, topography may under certain circumstances provide the possibility of multiple equilibria (Charney and DeVore 1979). Since the pioneering work of Charney and DeVore (1979) the idea of multiple equilibria was introduced into the context of blocking, namely, the coexistence of a normal small-amplitude state and a large-amplitude state reminiscent of blocking systems. As mentioned above, the importance of topographic forcing for atmospheric blocking has since been queried. In particular, for low-order models it is argued that multiple equilibria may be an artifact of the truncation; see, for example, Tung and Rosenthal (1985), Cehelsky and Tung (1985), and Yano and Mukougawa (1992). Nevertheless, the idea of multiple equilibria has remained intriguing and promising. And indeed, in our previous paper we were able to present a model in which multiple equilibria occur even in the absence of topographic forcing.

In this paper we demonstrate that, consistent with observations (i.e., Egger et al. 1986), topography is not necessary to support blocking systems but may provide an environment for its enhanced generation and development. We show that topographic forcing, indeed, does support the same type of solutions as in the nontopographic case studied in GG, but may additionally lead to larger amplitudes, multiple equilibria, and trapped waves. All these features are suggestive of blocking systems.

To overcome the unrealistic assumption of global topographic theories (for instance, Charney and DeVore 1979) such as periodicity and nonlocality, Patoine and Warn (1982) and Warn and Brasnett (1983) introduced local models describing the interaction of solitary waves with localized topographic features. In a similar manner Mitsudera and Grimshaw (1991, 1994) investigated related phenomena in the oceanographic environment. Continuing our previous work (GG) in the same spirit, we will derive here a pair of coupled Korteweg–de Vries equations, obtain and analyze some steady-state solutions, and relate these to blocking systems.

2. Weakly nonlinear, long-wave approximation

We proceed as in GG. Thus, we take a quasigeostrophic two-layer model on a β plane. We shall use a nondimensional coordinate system, based on a typical horizontal lengthscale L; a typical vertical scale for each layer D_1, D_2 with $H_0 = D_1 + D_2$; and typical Coriolis parameter f_0. A typical velocity U is taken to be the maximum of the mean current velocity and the timescale is given by U/L. We obtain the following equations (Pedlosky 1987) for the nondimensional pressure fields p_1 and p_2:

$$\left(\frac{\partial}{\partial t} - p_{1y}\frac{\partial}{\partial x} + p_{1x}\frac{\partial}{\partial y}\right) \times [\nabla^2 p_1 + \beta y + F_1(p_2 - p_1)] = 0,$$

$$\left(\frac{\partial}{\partial t} - p_{2y}\frac{\partial}{\partial x} + p_{2x}\frac{\partial}{\partial y}\right) \times [\nabla^2 p_2 + \beta y + F_2(p_2 - p_1) + \eta_B] = -\frac{E_V^{1/2}}{2\epsilon}\Delta p_2, \tag{2.1}$$

with the boundary conditions

$$p_{1,2} = \text{const} \quad \text{at } y = -L,\ 0. \tag{2.2}$$

Here the pressure fields are scaled by $\rho_{1,2} f_0 U_0 L_0$ and, in this quasigeostrophic approximation, also serve as streamfunctions for the velocity fields in each layer. The subscripts 1 and 2 are associated with the upper and lower layers, respectively, with $\rho_{1,2}$ being the density of the upper (lower) layer. We have introduced the nondimensional meridional gradient of planetary vorticity β; the Rossby number $\epsilon = U_0/f_0 L_0$ ($\epsilon \ll 1$ in the quasigeostrophic approximation); the vertical Ekman number E_V, which is $O(\epsilon^2)$; the topographic feature $h_B = \epsilon D_2 \eta_B$; and the Froude numbers $F_n = (L_0/R_i)^2$, where R_i is the internal Rossby radius of deformation for each layer, that is, $R_i = f_0^{-1}\sqrt{gD_n(\rho_2 - \rho_1)/\rho_2}$. It is pertinent to mention that very similar equations [(2.1)] hold if surface heating is considered instead of topography. The concept of surface heating acting as ''equivalent orography'' has been pointed out in Fandry and Leslie (1984), Dickinson (1978), and Davey (1981).

If we separate the mean currents, which are assumed to depend on y only, from the perturbation field, so that

$$p_{1,2} = -\int_{-L}^{y} U_{1,2}(y')\, dy' + \psi_{1,2}(x, y), \tag{2.3}$$

we can perform a weakly nonlinear long-wave analysis and derive an evolution equation for the perturbation field ψ_i. The procedure is described in detail in GG, but for convenience it is summarized here in the appendix. The outcome is that the perturbation field, to the leading order, is given by

$$\psi_i^{(0)}(X, T, y) = A_i(X, T)U_i^{(0)}(y). \tag{2.4}$$

Thus the meridional structure of ψ_i is entirely determined by the mean currents at this order. At the next order we obtain a pair of coupled Korteweg–de Vries equations for the rescaled amplitudes A_i:

$$A_{1T} + \Delta_1 A_{1X} - 6\mu A_1 A_{1X} - \lambda A_{1XXX} - \kappa_1 A_{2X} = 0,$$
$$A_{2T} + \Delta_2 A_{2X} - 6A_2 A_{2X} - A_{2XXX} - \kappa_2 A_{1X} = D_X - EA_2. \tag{2.5}$$

The definition of the parameters in (2.5) are given in the appendix.

For the nondissipative case ($E = 0$) there exists a conserved Hamiltonian for the full system of coupled KdV equations (2.5). Indeed, they can then be written as a noncanonical Hamiltonian system,

$$A_{1t} = -\partial_x \frac{1}{\kappa_2}\left(\frac{\delta \mathcal{H}}{\delta A_1}\right) \quad \text{and} \quad A_{2t} = -\partial_x \frac{1}{\kappa_1}\left(\frac{\delta \mathcal{H}}{\delta A_2}\right),$$

where δ denotes the functional derivative and $\mathcal{H}$ is the Hamiltonian density, which is found to be

$$\mathcal{H} = \kappa_2\left(\frac{1}{2}\Delta_1 A_1^2 - \mu A_1^3 + \frac{\lambda}{2}A_{1x}^2\right) + \kappa_1\left(\frac{1}{2}\Delta_2 A_2^2 - A_2^3 + \frac{1}{2}A_{2x}^2 - DA_2\right) - \kappa_1\kappa_2 A_1 A_2.$$

Due to the skew-symmetric operator ∂_x the Hamiltonian $H = \int_{-\infty}^{\infty} \mathcal{H}\, dx$ is conserved. Also, since $E = 0$ there are two Casimirs $\int_{-\infty}^{\infty} A_1\, dX$ and $\int_{-\infty}^{\infty} A_2\, dX$.

An equation for the energy of the full nonlinear equations (2.5) can be obtained by multiplying the first equation of (2.5) with A_1 and the second equation with A_2 and integrating over the whole domain. After integration by parts, we obtain

$$\begin{aligned}\frac{1}{2}\frac{d}{dt}\int_{-\infty}^{+\infty} A_1^2\, dX &= \kappa_1 \int_{-\infty}^{+\infty} A_1 A_{2X}\, dX \\ \frac{1}{2}\frac{d}{dt}\int_{-\infty}^{+\infty} A_2^2\, dX &= -\kappa_2 \int_{-\infty}^{+\infty} A_1 A_{2X}\, dX \\ &\quad + \int_{-\infty}^{+\infty} D_X A_2\, dX - E\int_{-\infty}^{+\infty} A_2^2\, dX,\end{aligned} \tag{2.6}$$

and so

$$\frac{d}{dt}\left(\kappa_2 \int_{-\infty}^{+\infty} A_1^2\, dX + \kappa_1 \int_{-\infty}^{+\infty} A_2^2\, dX\right) = 2\kappa_1 \int_{-\infty}^{+\infty} A_2 D_X\, dX - 2\kappa_1 E \int_{-\infty}^{+\infty} A_2^2\, dX. \tag{2.7}$$

For the nondissipative, nontopographic case one can derive a stability criterion from this energy equation, which, as shown in GG, is equivalent to the Charney–Stern condition for baroclinic instability. It is readily shown from (2.7) that

$$\kappa_1\kappa_2 < 0 \tag{2.8}$$

is a necessary condition for baroclinic instability. In terms of a long-wave approximation of (2.5) the instability criterion (2.8) can be further refined to $|\Delta_2 - \Delta_1 + \delta c_2 - \delta c_1| < 2\sqrt{-\kappa_1\kappa_2}$, where δc_i are the dispersive phase speed corrections.

In the absence of topographic forcing and damping (i.e., $D = 0$ and $E = 0$) the system (2.5) supports an explicit solitary-wave solution of the form

$$A_i = a_i \operatorname{sech}^2(w(X - cT)), \tag{2.9}$$

with the following relations for the parameters:

$$a_1 = 2\frac{\lambda}{\mu}w^2, \qquad a_2 = 2w^2, \tag{2.10}$$

and

$$c = \Delta_1 - 4\lambda w^2 - \kappa_1\frac{\mu}{\lambda} = \Delta_2 - 4w^2 - \kappa_2\frac{\lambda}{\mu}. \tag{2.11}$$

Note that Eq. (2.11) determines the allowed values for the coupling parameters κ_i and the linear phase velocities Δ_i needed to keep w^2 positive. An asymptotic perturbation theory performed in GG showed that the solitary-wave solution (2.9) is stable if $\kappa_1\mu < 0$ or unstable if $\kappa_1\mu > 0$. However, as discussed more fully in GG, we note here that instability of a solitary wave may merely imply separation of the upper- and lower-layer waves and is not related to the linear instability criterion (2.8). Indeed, we can show that there are no unstable solitary waves of the form (2.9) when the background is linearly unstable. That is, $\kappa_1\mu < 0$, together with $\kappa_1\kappa_2 < 0$, implies that $(\Delta_2 - \Delta_1)^2 + 4\kappa_1\kappa_2 > 0$ when (2.11) holds.

In section 3 we will solve steady-state solutions of the system (2.5) by performing an asymptotic perturbation theory, and investigate their stability. In section 4 we will simulate the pair of coupled KdV equations (2.5) numerically. In section 5 we discuss the results obtained by our asymptotic theory and test the validity of the long-wave approximation by simulating the full topographically forced quasigeostrophic two-layer system (2.1) using the approximative solutions of the system (2.5) derived in section 2 as initial conditions.

3. Asymptotic approximation

a. Introduction

In this section we use an asymptotic approximation that assumes weak coupling, friction, and topographic forcing. The essence of this approach is to assume that the effect of the small perturbations is only to modify the solitary-wave parameters, namely, amplitude and phase, of the undisturbed, uncoupled KdV equations on a slow timescale. Thus we assume that each solitary wave has a slowly varying time-dependent amplitude and phase, and obtain ordinary differential equations describing the time evolution of these parameters. This method was introduced by Johnson (1973), Karpman and Maslov (1978), and Kaup and Newell (1978) for a single KdV equation. An extension to this work was made by Grimshaw and Mitsudera (1993) using a multiscale perturbation expansion to take into account higher-order terms. We will follow this approach and use the resulting amplitude and phase equations to extract

information about solutions of the system of coupled KdV equations (2.5). In particular, we will be able to discuss the stability properties of steady-state solutions. Again the reader is referred to GG for a more detailed discussion of the asymptotic development.

b. Asymptotic analysis

We recall the system of coupled KdV equations (2.5)

$$A_{1t} + \Delta_1 A_{1x} - 6\mu A_1 A_{1x} - \lambda A_{1xxx} - \epsilon\kappa_1 A_{2x} = 0,$$
$$A_{2t} + \Delta_2 A_{2x} - 6A_2 A_{2x} - A_{2xxx} + \epsilon(-\kappa_2 A_{1x} - D_x + EA_2) = 0, \quad (3.1)$$

where, for convenience, we have introduced a small parameter $\epsilon \ll 1$ and have assumed that κ_1, κ_2, E, and D are $O(\epsilon)$. Later on, we will restore the original parameters back into the final differential equations. As discussed above, the influence of the perturbation is to modify the amplitude and phase of the unperturbed KdV solitary waves (2.9) on a slow timescale $T = \epsilon t$. Thus we seek an asymptotic expansion of the form

$$A_1 = u_0 + \epsilon u_1 + \epsilon^2 u_2 + \cdots$$
$$A_2 = v_0 + \epsilon v_1 + \epsilon^2 v_2 + \cdots$$
$$u_0 = a_1(T)\,\mathrm{sech}^2(w_1(T)(x - \Phi_1(T)))$$
$$v_0 = a_2(T)\,\mathrm{sech}^2(w_2(T)(x - \Phi_2(T)))$$
$$\Phi_i = \frac{1}{\epsilon}\int_0^T c_i(T')\,dT' \qquad i = 1, 2$$
$$c_i = c_i^{(0)} + \epsilon c_i^{(1)} + \cdots \qquad i = 1, 2. \quad (3.2)$$

Substitution of these expansions into Eq. (3.1) yields at the leading order the well-known solitary-wave solutions of the undisturbed uncoupled KdV equation provided that

$$a_1 = 2\frac{\lambda}{\mu}w_1^2, \qquad a_2 = 2w_2^2. \quad (3.3)$$

At the next order, $O(\epsilon)$, time evolution equations for the amplitudes and phases are obtained. At the second order, $O(\epsilon^2)$, one obtains the first-order speed corrections. Restoring the original version of the parameters κ_1, κ_2, E, and D we summarize the results:

$$\frac{da_1}{dt} = -2\kappa_1 a_2 w_2 \int_{-\infty}^{\infty} \mathrm{sech}^2(\psi)\,\mathrm{sech}^3\left(\frac{w^2}{w_1}\psi - w_2\Delta\Phi\right)\sinh\left(\frac{w_2}{w_1}\psi - w_2\Delta\Phi\right)d\psi,$$

$$\frac{da_2}{dt} = -2\kappa_2 a_1 w_1 \int_{-\infty}^{\infty} \mathrm{sech}^2(\psi)\,\mathrm{sech}^3\left(\frac{w^1}{w_2}\psi + w_1\Delta\Phi\right)\sinh\left(\frac{w_1}{w_2}\psi + w_1\Delta\Phi\right)d\psi - \frac{4}{3}Ea_2$$
$$+ w_2\int_{-\infty}^{\infty}\mathrm{sech}^2(w_2\psi)D_\psi(\psi + \Phi_2)\,d\psi,$$

$$\frac{d\Phi_1}{dt} = \Delta_1 - 2\mu a_1 - \kappa_1\frac{\mu}{\lambda}\frac{w_2^3}{w_1^3}\int_{-\infty}^{\infty}[\tanh(\psi) + \psi\,\mathrm{sech}^2(\psi) - \mathrm{sign}(\lambda)\tanh^2(\psi)]\,\mathrm{sech}^2\left(\frac{w_2}{w_1}\psi - w_2\Delta\Phi\right)$$
$$\times \tanh\left(\frac{w^2}{w_1}\psi - w_2\Delta\Phi\right)d\psi,$$

$$\frac{d\Phi_2}{dt} = \Delta_2 - 2a_2 - \kappa_2\frac{\lambda}{\mu}\frac{w_1^3}{w_2^3}\int_{-\infty}^{\infty}[\tanh(\psi) + \psi\,\mathrm{sech}^2(\psi) - \tanh^2(\psi)]\,\mathrm{sech}^2\left(\frac{w_1}{w_2}\psi + w_1\Delta\Phi\right)$$
$$\times \tanh\left(\frac{w^1}{w_2}\psi + w_1\Delta\Phi\right)d\psi$$
$$+ \frac{1}{2a}\int_{-\infty}^{\infty}[\tanh(w_2\psi) + w_2\psi\,\mathrm{sech}^2(w_2\psi) - \tanh^2(w_2\psi)] \times D_\psi(\psi + \Phi_2)\,d\psi - \frac{E}{3w_2}, \quad (3.4)$$

where $\Delta\Phi = \Phi_2 - \Phi_1$. The amplitude equations contain the leading-order energy balance, as can be seen by inserting u_0 and v_0 into the full nonlinear energy equations (2.7). We note that the ''$\tanh^2$'' terms in the interaction integrals of the equations describing the time evolution of the phases $\Phi_{1,2}$ are the contribution of the radiating tails to the first-order speed corrections.

c. Steady-state solutions and multiple equilibria

In the nondissipative, unforced case the system of equations (3.4) supports the steady-state solution, namely, $w_1 = w_2 = w^*$, $a_1 = a_1^* = 2\lambda w^{*2}/\mu$, $a_2 = a_2^* = 2w^{*2}$ with

$$\Delta\Phi^* = 0 \tag{3.5}$$

$$\Delta_2 - \Delta_1 - 4(1-\lambda)w^{*2} - \kappa_2\frac{\lambda}{\mu} + \kappa_1\frac{\mu}{\lambda} = 0. \tag{3.6}$$

Note that this is exactly the condition (2.11) previously found for $D = 0$. But we should note that there might also be solutions of (3.4) with $w_1^* \neq w_2^*$ that are not apparent in the full coupled KdV equations. We will investigate these extraneous solutions in section 3e.

The condition $\Delta\Phi = 0$ assures that the two waves of the coupled layers are locked together. If topography is present, the steady-state waves must also stay locked to the topography, and we will get the additional constraint $\Phi_1 = \Phi_2 = 0$. The condition for steady-state solutions determining the amplitudes now allows for the possibility of multiple equilibria when topography is included. The multiple equilibria are states where there is more than one possible value of the amplitudes for the same set of parameters.

In order to keep the system as simple as possible we restrict ourselves to a symmetric topographic feature. All symmetric topographic features support steady-state solutions with $\Phi_2 = 0$, whereas this is not generally the case for asymmetric topographic features, as can be seen from the amplitude equation (3.4) for a_2. We note that for simplicity from this point on we do not consider surface heating anymore. Sea surface heating would require asymmetric shapes of the equivalent orography and, hence, would cause the algebra to be rather awkward.

If an explicit expression is needed, we represent the topography by a ''sech^2'' profile according to

$$D(x) = D_0\,\mathrm{sech}^2\left(\frac{x}{p}\right),$$

where p is a measure for the width of the topographic feature. Other analogous expressions could be used and would yield similar results. The topographic interaction integrals of the reduced system (3.4) can be simplified in the limiting cases $p \ll 1$ and $p \gg 1$, that is, in the limit of narrow and broad topographic features, respectively.

In the case of a narrow topographic feature, $D(x)$ acts like a δ function and the interaction integral appearing in the amplitude equation of (3.4) reduces to

$$w_2\int_{-\infty}^{\infty}\mathrm{sech}^2(w_2\psi)D_\psi(\psi+\Phi_2)\,d\psi \approx -2a_2pD_0\,\mathrm{sech}^2(w_2\Phi_2)\tanh(w_2\Phi_2), \tag{3.7}$$

where

$$2pD_0 = \int_{-\infty}^{\infty} D(\psi)\,d\psi,$$

and the contribution to the first-order speed correction in the equation for Φ_2 reduces to

$$\frac{1}{2a_2}\int_{-\infty}^{\infty} D_\psi(\psi+\Phi_2)[\cdots]\,d\psi \approx -\frac{pD_0}{w_2}[\mathrm{sech}^2(w_2\Phi_2) - w_2\Phi_2\,\mathrm{sech}^2(w_2\Phi_2) \times \tanh(w_2\phi_2)]. \tag{3.8}$$

For the case of a broad topographic feature the solitary wave may be approximated by a δ function and we can simplify the topographic interaction integral in the amplitude equation as

$$w_2\int_{-\infty}^{\infty}\mathrm{sech}^2(w_2\psi)D_\psi(\psi+\Phi_2)\,d\psi \approx 2D_{\Phi_2}(\Phi_2), \tag{3.9}$$

and the interaction integral of the phase equation as

$$\frac{1}{2a_2}\int_{-\infty}^{\infty} D_\psi(\psi+\Phi_2)[\cdots]\,d\psi \approx -\frac{1}{a_2}D(\Phi_2). \tag{3.10}$$

Note that in both these limits, we do not need to use the explicit representation (3.7) for the topography.

In the topographically forced KdV equation we can obtain multiple equilibria as discussed in Warn and Brasnett (1983) and Grimshaw et al. (1995), among others. This is not possible here for a fixed set of parameters since the solitary wave is not only locked to the topography but also to the other layer, which breaks the single constraint $\Delta\Phi = 0$ into $\Phi_1 = \Phi_2 = 0$. Hence, instead of the one equation (3.5), one obtains two equations as a condition for steady states, namely,

$$\Delta_1 - 4\lambda w^{*2} - \kappa_1\frac{\mu}{\lambda} = 0 \tag{3.11}$$

and

$$\Delta_2 - 4w^{*2} - \kappa_2\frac{\lambda}{\mu} - \frac{p}{w^*}D_0 = 0 \tag{3.12}$$

for a narrow topography, or

$$\Delta_2 - 4w^{*2} - \kappa_2\frac{\lambda}{\mu} - \frac{1}{2w^{*2}}D_0 = 0 \tag{3.13}$$

for a broad topography. Indeed, the amplitude is uniquely determined by (3.11).

However, if we allow Δ_1 and Δ_2 to be free parameters, which can be achieved by introducing a small inhomogeneity to the mean flow according to the definition of the parameters (A.15) as discussed in the appendix, we may obtain multiple equilibria. In Fig. 1 we have depicted the steady-state amplitude $2w^{*2}$ as a function of $\Delta := (-\Delta_2 + \kappa_2\lambda/mu)/4$ as determined by the condition for a broad topographic feature [(3.13)].

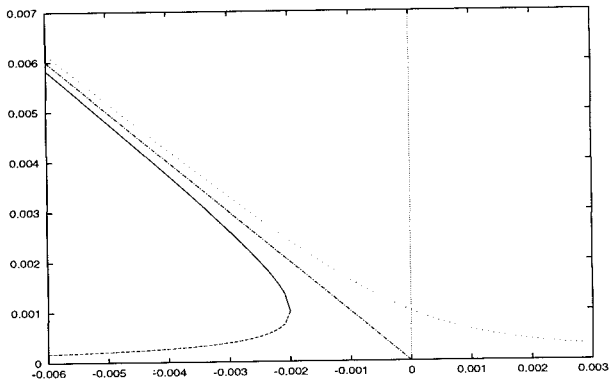

FIG. 1. Plot of an equilibrium state [(3.12) or (3.13)]. Continuous (dotted) line for $D_0 > 0$ or <0, respectively. The straight line depicts the nontopographic case.

For $D_0 > 0$ there is one solution for every Δ, shown as the upper branch of Fig. 1. For $D_0 < 0$ we obtain the lower branch of Fig. 1 and obtain two solutions if $\Delta < -\sqrt{D_0/2}$. In particular, we obtain one large-amplitude state and one small-amplitude state. For the narrow topography the picture looks qualitatively the same as in Fig. 1 and analogous expressions can be found for the two branches. We note that for small μ only a slight shift in Δ_1 is required to allow for the two amplitude states. Note also that in the case of a broad topographic feature the condition for steady states [(3.13)] is independent of the width and only depends on the height of the topography as can be seen from (3.10).

Next we include friction, which leads to the possibility of multiple equilibria associated with a balance between dissipation and forcing in the amplitude equation for a_2. In this case the multiple equilibria do not consist of states of different amplitudes but of states of different locations. In particular, the amplitude a_2 is just that of a stationary solution, that is, satisfying $\Delta_1 - 2\mu a_1^* = 0$ and $\Delta_2 - 2a_2^* = 0$ if we neglect first-order corrections, but the amplitude equation determines now the number of possible states and their position Φ_2. The balance determining Φ_2 is written as

$$\frac{4}{3}Ea_2^* = w_2 \int_{-\infty}^{\infty} \operatorname{sech}^2(w_2\psi) D_\psi(\psi + \Phi_2)\, d\psi \quad (3.14)$$

and can be simplified using (3.7) or (3.9). We find that there are no multiple equilibria possible for $D_0 > \sqrt{3}E/p$ in the case of narrow topography and for $D_0 > \sqrt{3}Epa_2/2$ in the case of broad topography. This implies that for fixed dissipation a broad (narrow) topographic feature has to be larger the broader (narrower) it is to support multiple equilibria. Figure 2 depicts the conditions (3.14). For positive forcing $D_0 > 0$ the two states have $\Phi_2 < 0$ and are attached to the western side of the topographic feature; for negative forcing $D < 0$ the two states have $\Phi_2 > 0$ and are attached to the eastern side of the topographic feature. We observe that for more complicated topographic features the number and location of possible states is associated with the number of extremes of D_ψ. Figure 2 also helps to interpret the two solutions for $E \neq 0$ and to understand where they come from. This is seen for small E, that is, when the dashed line in Fig. 2 is close to the Φ_2 axis; one solution arises from the topographic solution at $\Phi_2 = 0$, the other solution comes from the free solitary-wave solution at $\Phi_2 = -\infty$ where the solitary wave does not feel the topography. The influence of dissipation is to link these two distinct, independent solutions.

d. Stability analysis

For the moment we will again restrict ourselves to the nondissipative case, where we have the steady state $(a_1^*, a_2^*, \Phi_1^*, \Phi_2^*)$, namely,

$$\Delta\Phi^* = 0, \qquad \Phi_1^* = \Phi_2^* = 0,$$

$$\Delta_1 - 2\mu a_1^* - \kappa_1 \frac{\mu}{\lambda} = 0,$$

$$\Delta_2 - 2a_2^* - \kappa_2 \frac{\lambda}{\mu} + \frac{1}{2a_2^*} \times \int_{-\infty}^{\infty} [\tanh(w_2^*\psi) + w_2^*\psi \operatorname{sech}^2(w_2^*\psi)] D_\psi(\psi)\, d\psi = 0. \quad (3.15)$$

We perform a linear stability analysis by linearization about this steady state, that is, we write

$$\Phi_1 = \Phi_1^* + \delta\varphi_1, \qquad \Phi_2 = \Phi_2^* + \delta\varphi_2,$$
$$a_1 = a_1^* + \delta a_1, \qquad a_2 = a_2^* + \delta a_2. \quad (3.16)$$

After some algebra we obtain

$$\delta\dot{a}_1 = \frac{8}{15}\kappa_1 a_2^{*2}\delta\Delta\varphi$$

$$\delta\dot{a}_2 = -\frac{8}{15}\kappa_2\frac{\mu}{\lambda}a_1^{*2}\delta\Delta\varphi + C_1(D)\delta\varphi_2$$

$$\delta\dot{\varphi}_1 = \left[-2\mu + \left(\frac{2}{3} + \frac{\pi^2}{45}\right)\kappa_1\frac{\mu}{\lambda}\frac{1}{a_1^*}\right]\delta a_1 - \left(\frac{2}{3} + \frac{\pi^2}{45}\right)\kappa_1\frac{1}{a_1^*}\delta a_2^* - \frac{8}{15}r_1\kappa_1\frac{\mu}{\lambda}w^*\delta\Delta\varphi$$

$$\delta\dot{\varphi}_2 = \left[-2 + \left(\frac{2}{3} + \frac{\pi^2}{45}\right)\kappa_2\frac{\lambda}{\mu}\frac{1}{a_2^*} + C_2(D)\right]\delta a_2 - \left(\frac{2}{3} + \frac{\pi^2}{45}\right)\kappa_2\frac{1}{a_2^*}\delta a_1^* + \frac{8}{15}r_2\kappa_2\frac{\lambda}{\mu}w^*\delta\Delta\varphi, \quad (3.17)$$

where the dot denotes the time derivative and the constants C_i are given by

$$C_1(D) = w^* \int_{-\infty}^{\infty} D_{\psi\psi}(\psi)\,\mathrm{sech}^2(w^*\psi)\,d\psi,$$

$$C_2(D) = \frac{w^*}{a_2^{*2}} \int_{-\infty}^{\infty} [\mathrm{sech}^2(w^*\psi) - w^*\psi\,\mathrm{sech}^2(w^*\psi)\,\tanh(w^*\psi)]D(\psi)\,d\psi + \frac{1}{2a_2^{*2}} \int_{-\infty}^{\infty} [w^*\psi\,\mathrm{sech}^2(w^*\psi) - (w^*\psi)^2\,\mathrm{sech}^2(w^*\psi)\,\tanh(w^*\psi)]D_{\psi}(\psi)\,d\psi. \quad (3.18)$$

For a narrow topographic feature the coefficients $C_{1,2}(D)$ are simplified to

$$C_1(D) = -2pD_0a_2^*w^*, \qquad C_2(D) = \frac{pw^*}{a_2^{*2}}D_0. \quad (3.19)$$

For a broad topography we find

$$C_1(D) = -\frac{4}{p^2}D_0, \qquad C_2(D) = \frac{1}{a_2^{*2}}D_0. \quad (3.20)$$

This can be obtained either via linearizing (3.7), (3.8), or (3.9), (3.10), or by going into the Eq. (3.18) with the approximations of either a narrow or broad topography.

We set $\delta a_1 = \delta a_1^{(0)} \exp(\gamma t)$, $\delta a_2 = \delta a_2^{(0)} \exp(\gamma t)$, etc., and obtain (omitting the superscripts) a system of linear equations,

$$\begin{pmatrix} 0 \\ 0 \\ 0 \\ 0 \end{pmatrix} = \begin{pmatrix} -\gamma & 0 & -\xi & \xi \\ 0 & -\gamma & -\rho & \rho + \zeta \\ \alpha & \beta & -\sigma - \gamma & \sigma \\ \epsilon & \eta & -\theta & \theta - \gamma \end{pmatrix} \begin{pmatrix} \delta a_1 \\ \delta a_2 \\ \delta\varphi_1 \\ \delta\varphi_2 \end{pmatrix}, \quad (3.21)$$

where the matrix elements are defined by (3.17). The solvability condition reads as

$$\gamma^4 + \gamma^3(\sigma - \theta) + \gamma^2[\xi(\alpha - \epsilon) + \rho(\beta - \eta) - \zeta\eta] + \gamma(-\zeta\beta\theta - \zeta\eta\sigma) - \xi\zeta(\alpha\eta - \epsilon\beta) = 0. \quad (3.22)$$

If we include all effects we have an effective four-dimensional phase space with, in general, four distinct eigenvalues γ, which can be either real or complex valued. Thus our full system contains the possibility of chaos. Note that odd powers of γ are associated with the radiation coefficients σ and θ. Incidentally, we note that if we were able to find an odd topographic feature supporting a steady-state solution of (3.4), which as mentioned above is not generally the case, the contributions of such a topography (e.g., surface heating) would also appear in the odd powers of γ in (3.22). It is pertinent to mention that we will talk here about instability not in the nonlinear sense of baroclinic instability as derived in Eq. (2.8) from the full coupled Korteweg–deVries equations but in the sense of the solitary wave as a steady-state solution of the reduced amplitude and phase equations (3.4). These reduced equations contain an equation for the phase, that is, the location of the solitary wave, and involve phase separation. This allows a solution of (3.4) to be an unstable saddle point without infinite growth of the amplitudes but instead a growth of the phase separation. In the nonlinear criterion for instability of the coupled KdV equations (2.5) we have integrated over the spatial domain and thus cannot obtain this kind of instability.

For the nontopographic case the phase plane is effectively two-dimensional and we recall the results derived in GG. If one omits the first-order speed corrections, the system (3.4) supports either a stable center or a saddle point, depending on the sign of $\kappa_1\mu$. In particular, the solitary wave is stable if $\kappa_1\mu < 0$ and corresponds to a center, and is unstable otherwise, corresponding to a saddle point.

The physical meaning of the sign combination of $\kappa_1\mu$ was interpreted in GG as a condition for a spatially slightly perturbed steady-state solution to change its amplitude in such a way that the associated change in the phase velocity forces the solitary wave to relax back to the equilibrium position, or to separate further. It seems, therefore, that it is not enough to look at the Charney–Stern condition for baroclinic instability (2.8) with respect to blocking but one also has to take into account this additional criterion involving $\kappa_1\mu$. The first-order speed corrections, which will become important for small amplitudes, have a stabilizing effect on the dynamics. Radiation, in the absence of topography, does not change the effective dimension of the phase plane. Its effect is to convert a center into a stable focus and to enhance the growth rates of a saddle point.

In the case of a topographic feature, which is even with respect to the solitary wave of the lower layer, we find for the growth rate on neglecting the effect of radiation,

$$\gamma^4 + \gamma^2[\xi(\alpha - \epsilon) + \rho(\beta - \eta) - \zeta\eta] - \xi\zeta(\alpha\eta - \epsilon\beta) = 0. \quad (3.23)$$

This invokes locally the dynamics to be constrained to two crossing planes in the four-dimensional phase plane. Radiation will, in this case, destroy the constraints, and leads to the full four-dimensional phase space. To simplify further we also omit the first-order speed corrections arising from the coupling, in particular β and ϵ; hence, we get

$$\gamma^4 + \gamma^2(\xi\alpha - \rho\eta - \zeta\eta) - \xi\zeta\alpha\eta = 0. \quad (3.24)$$

Equations (3.23) and (3.24) are of the form $\gamma^4 + a\gamma^2$

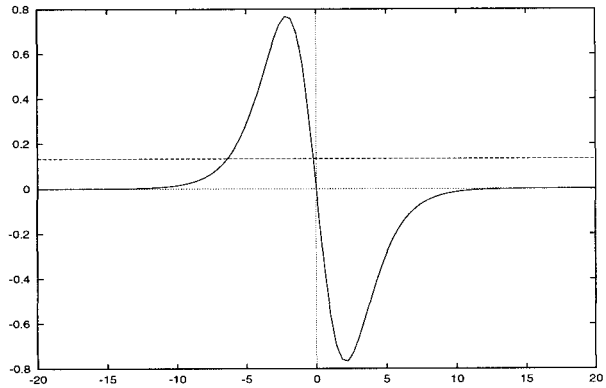

FIG. 2. Schematic visualization of the condition (3.14). Plotted is the amplitude $2w^{*2}$ against Φ_2. The equilibrium points Φ_2 are found as the points of intersection of the two curves. Here a case for positive D_0 is given.

$+ b = 0$, and hence allow three different stability scenarios. In particular, for $a > 0$, $0 < b < a^2/4$ there are only purely imaginary solutions for γ corresponding to stability; for $a < 0$, $0 < b < a^2/4$ there are only purely real solutions corresponding to instability; and for all other cases we have complex-valued solutions for γ, again representing instability.

We will discuss the stability properties of the solitary wave for the case of a narrow topography by varying D_0. Again the crucial parameter determining the stability is the sign of $\kappa_1\mu$. If we neglect all first-order speed corrections, that is, set $\alpha = -2\mu$ and $\eta = -2$, the plots for γ as a function of D_0 are shown in Fig. 3. For $\kappa_1\mu < 0$ we have purely imaginary solutions for $D_0 < 0$, and two real solutions for $D_0 > 0$. For $\kappa_1\mu > 0$ one can show that there are two real solutions for $D_0 < 0$ and four real solutions for $D_0 > 0$. For either sign of $\kappa_1\mu$ we find $\gamma \sim |D_0|$ for large $|D_0|$.

If we include the topographic first-order speed-correction term, which as we have seen above gives rise to multiple equilibria, but neglect the first-order speed correction terms due to the coupling, the scenarios are again generic and are shown in Fig. 4. The general effect of the topographic speed correction is stabilizing. For $\kappa_1\mu < 0$ the solution becomes stable for $D_0 > 4wa_2/p$. Similar stabilizing effects also occur for $\kappa_1\mu > 0$ where for $D_0 > 4wa_2/p$ there are only two real solutions compared to four in the previous case.

Again we can interpret the stability criteria in the same manner as in GG for the sign of $\kappa_1\mu$ by looking at the changes in the solitary-wave speed associated with the changes in the amplitude of the solitary wave induced by the topographic forcing. In this sense stability means that the change in the solitary-wave speed is such that the solitary wave is forced to return to its equilibrium position. To filter out the purely topographic effect we shall ignore the coupling and only consider the forced lower layer. Using (3.8) or (3.10) the condition for stability in this sense for a solitary wave with $a_2 > 0$ displaced to the right from its equilibrium position, which is centered over the topography, reads as

$$\Delta_2 - 2[a_2^* - \text{sign}(D_0)\delta a] - \frac{\sqrt{2}p}{\sqrt{a_2^* - \text{sign}(D_0)\delta a}}D_0 < \Delta_2 - 2a_2^* - \frac{\sqrt{2}p}{\sqrt{a_2^*}}D_0 = 0 \tag{3.25}$$

for narrow topography, and

$$\Delta_2 - 2[a_2^* - \text{sign}(D_0)\delta a] - \frac{1}{a_2^* - \text{sign}(D_0)\delta a}D_0 < \Delta_2 - 2a_2^* - \frac{1}{a_2^*}D_0 = 0 \tag{3.26}$$

for broad topography. If we linearize around the equilibrium state we obtain the following inequalities:

$$\text{sign}(D_0)D_0 > 4a_2^*\frac{p}{w^*}\,\text{sign}(D_0) \tag{3.27}$$

for narrow topography, and

$$\text{sign}(D_0)D_0 > 2a_2^*\,\text{sign}(D_0) \tag{3.28}$$

for broad topography. This is exactly the condition for stability as found above; that is, we have an unstable band for $0 < D_0 < 4a_2^*w^*/p$ for broad topography.

If we include all first-order speed corrections, that is, solve equation (3.23) in full, the situation gets more complicated and depends on the amplitudes $a_{1,2}$. For $\kappa_1\mu > 0$ the interesting case of a stable gap for $0 > D_0 > D_0^*$ is possible, revealing the stabilizing

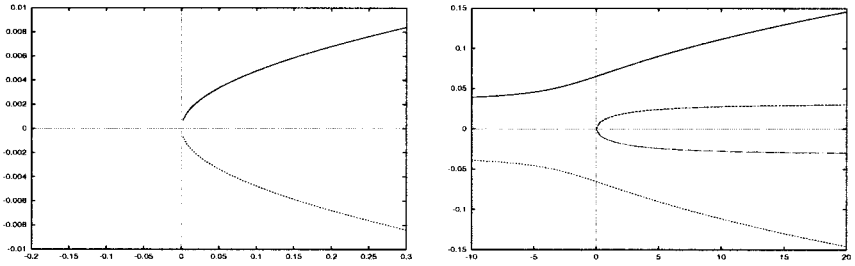

FIG. 3. Generic plot of the real part of γ vs D_0 when all first-order speed-correction terms are excluded: (left) the case $\kappa_1\mu < 0$; (right) $\kappa_1\mu > 0$.

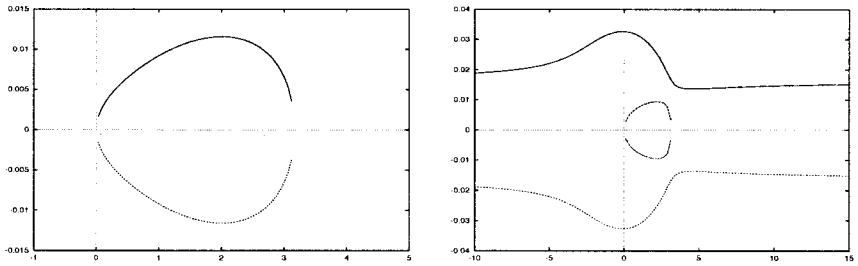

FIG. 4. Generic plot of the real part of γ vs D_0 when only topographic speed correction terms are included: (left) the case $\kappa_1\mu < 0$; (right) $\kappa_1\mu > 0$.

effect of the first order speed corrections as discussed above.

As we have shown in section 3c the balance of topographic forcing and frictional dissipation may lead to multiple equilibria for weak dissipation. We will now discuss the stability of these steady states with different phase locations. For simplicity we will restrict ourselves to the case of broad topography. If we linearize the system (3.4) around the steady-state solution, omitting first-order speed corrections, we obtain for the growth rate γ

$$\gamma^4 - e\gamma^3 + \gamma^2(\xi\alpha - \rho\eta - \zeta\eta) - e\alpha\xi\gamma - \xi\zeta\alpha\eta = 0, \tag{3.29}$$

where $e = -4E/3$ is the frictional contribution and $\zeta = 2D_{\psi\psi}(\Phi_2^*)$. We rewrite the equation (3.14) determining the equilibrium points Φ_2^* for the case of broad topography

$$2D_{\psi}(\Phi_2^*) = \frac{4}{3}Ea_2^*, \tag{3.30}$$

which is schematically depicted in Fig. 2. In the discussion above about the stability of topographic steady-state solutions we found that the sign of $\xi\zeta\alpha\eta$ is crucial for the stability. It is readily seen that ζ has a different sign for each of the two possible solutions of (3.30). As discussed in section 3c the two possible solutions in the dissipative case emerge from the free solitary wave and the topographic steady-state solution, respectively, from which they also inherit their stability properties.

e. Quasi-steady-state solutions

The reduced system (3.4) also supports, in contrast to the full system of coupled KdV equations (2.5), solutions for which $w_1 \neq w_2$. To obtain these extraneous steady-state solutions we use variational methods, exploiting the Hamiltonian structure of (2.5) as discussed in section 2.

If we insert our ansatz (3.2) for A_1 and A_2 in the Hamiltonian H and calculate the leading-order term, we can verify after some lengthy algebra that the reduced Hamiltonian is conserved under the flow defined by the reduced system (3.4) provided that the radiating terms are omitted. These are just the terms representing the contribution of the radiating tails to the first-order speed corrections. It is pertinent to mention that only the reduced system including the first-order speed corrections, but omitting the radiating tail terms, is Hamiltonian and thus integrable. But these speed-correction terms are only dynamically important for small amplitudes, as can be seen from (3.4).

If we perform a variational approach for the Hamiltonian under the assumption $w_1 = w_2$ and ignoring topography, we obtain the steady-state solution (2.10) with $\Delta\Phi = \Phi_1 = \Phi_2 = 0$. We could also look for solutions of the form (3.2) (i.e., u_0 and v_0), whose leading terms are solitary waves but with $w_1 \neq w_2$ and without making the assumption that $a_{1,2}$ are a priori related to $w_{1,2}$. In this case the reduced Hamiltonian is

$$H_{\mathrm{red}} = \kappa_2\left(\frac{2}{3}\Delta_1\frac{a_1^2}{w_1} - \frac{16}{15}\mu\frac{a_1^3}{w_1} + \frac{8}{15}\lambda a_1^2 w_1\right) + \kappa_1\left(\frac{2}{3}\Delta_2\frac{a_2^2}{w_2} - \frac{16}{15}\frac{a_2^3}{w_2} + \frac{8}{15}a_2^2 w_2\right)$$
$$- \kappa_1\kappa_2 a_1 a_2 \frac{1}{w_1}\int_{-\infty}^{\infty}\mathrm{sech}^2(z)\,\mathrm{sech}^2\left(\frac{w_2}{w_1}z - w_2\Delta\Phi\right)dz - \kappa_1 a_2\int_{-\infty}^{\infty}\mathrm{sech}^2[w_2(z-\Phi_2)]D(z)\,dz. \tag{3.31}$$

A variational approach again gives $\Delta\Phi = \Phi_1 = \Phi_2 = 0$ as a condition for steady-state solutions, but the relations (2.10) and (2.11), that is, the lowest-order approximations of the adiabatic analysis performed in section 2, are now replaced by

$$
\begin{aligned}
&a_1 - 2\frac{\lambda}{\mu}w_1^2 - \frac{15}{16}\frac{\kappa_1}{\mu}\frac{a_2}{a_1}\int_{-\infty}^{\infty}\operatorname{sech}^2(z)\operatorname{sech}^2\left(\frac{w_2}{w_1}z\right)dz + \frac{15}{4}\frac{\kappa_1}{\mu}\frac{a_2}{a_1}\frac{w_2}{w_1}\int_{-\infty}^{\infty}z\operatorname{sech}^2(z)\operatorname{sech}^2\left(\frac{w_2}{w_1}z\right)\tanh\left(\frac{w_2}{w_1}z\right)dz = 0\\
&a_2 - 2w_2^2 + \frac{15}{16}\kappa_2\frac{a_1}{a_2}\frac{w_2}{w_1}\int_{-\infty}^{\infty}\operatorname{sech}^2(z)\operatorname{sech}^2\left(\frac{w_2}{w_1}z\right)dz - \frac{15}{4}\kappa_2\frac{a_1}{a_2}\frac{w_2^2}{w_1^2}\int_{-\infty}^{\infty}z\operatorname{sech}^2(z)\operatorname{sech}^2\left(\frac{w_2}{w_1}z\right)\tanh\left(\frac{w_2}{w_1}z\right)dz\\
&\quad + \frac{15}{16}D_0\frac{w_2}{a_2}\int_{-\infty}^{\infty}\operatorname{sech}^2\left(\frac{z}{p}\right)\operatorname{sech}^2(w_2z)\,dz - \frac{15}{4}D_0\frac{w_2^2}{a_2}\int_{-\infty}^{\infty}z\operatorname{sech}^2\left(\frac{z}{p}\right)\operatorname{sech}^2(w_2z)\tanh(w_2z)\,dz = 0\\
&\Delta_1 - 2\mu a_1 - \frac{9}{8}\kappa_1\frac{a_2}{a_1}\int_{-\infty}^{\infty}\operatorname{sech}^2(z)\operatorname{sech}^2\left(\frac{w_2}{w_1}z\right)dz + \frac{3}{2}\frac{a_2}{a_1}\frac{w_2}{w_1}\int_{-\infty}^{\infty}z\operatorname{sech}^2(z)\operatorname{sech}^2\left(\frac{w_2}{w_1}z\right)\tanh\left(\frac{w_2}{w_1}z\right)dz = 0\\
&\Delta_2 - 2a_2 - \frac{3}{8}\kappa_2\frac{a_1}{a_2}\frac{w_2}{w_1}\int_{-\infty}^{\infty}\operatorname{sech}^2(z)\operatorname{sech}^2\left(\frac{w_2}{w_1}z\right)dz - \frac{3}{2}\kappa_2\frac{a_1}{a_2}\frac{w_2^2}{w_1^2}\int_{-\infty}^{\infty}z\operatorname{sech}^2(z)\operatorname{sech}^2\left(\frac{w_2}{w_1}z\right)\tanh\left(\frac{w_2}{w_1}z\right)dz\\
&\quad - \frac{3}{8}\frac{w_2}{a_2}D_0\int_{-\infty}^{\infty}\operatorname{sech}^2\left(\frac{z}{p}\right)\operatorname{sech}^2(w_2z)\,dz - \frac{3}{2}\frac{w_2^2}{a_2}D_0\int_{-\infty}^{\infty}z\operatorname{sech}^2\left(\frac{z}{p}\right)\operatorname{sech}^2(w_2z)\tanh(w_2z)\,dz = 0. \qquad (3.32)
\end{aligned}
$$

For the special case $w_1 \gg w_2$ these equations simplify to

$$
\begin{aligned}
a_1 &= 2\frac{\lambda}{\mu}w_1^2 + \frac{15}{8}\frac{\kappa_1}{\mu}\frac{a_2}{a_1}\\
a_2 &= 2w_2^2 - \frac{15}{8}\kappa_2\frac{a_1}{a_2}\frac{w_2}{w_1} + \frac{15}{8}\frac{D_0}{a_2}f\\
0 &= \Delta_1 - 2\mu a_1 - \frac{9}{4}\kappa_1\frac{a_2}{a_1}\\
0 &= \Delta_2 - 2a_2 - \frac{3}{4}\kappa_2\frac{a_1}{a_2}\frac{w_2}{w_1} - \frac{3}{4}\frac{D_0}{a_2}f, \qquad (3.33)
\end{aligned}
$$

and for $w_1 \ll w_2$ to

$$
\begin{aligned}
a_1 &= 2\frac{\lambda}{\mu}w_1^2 - \frac{15}{8}\frac{\kappa_1}{\mu}\frac{a_2}{a_1}\frac{w_1}{w_2}\\
a_2 &= 2w_2^2 + \frac{15}{8}\kappa_1\frac{a_1}{a_2} + \frac{15}{8}\frac{D_0}{a_2}f\\
0 &= \Delta_1 - 2\mu a_1 - \frac{3}{4}\kappa_1\frac{a_2}{a_1}\frac{w_1}{w_2}\\
0 &= \Delta_2 - 2a_2 - \frac{9}{4}\kappa_2\frac{a_1}{a_2} - \frac{3}{4}\frac{D_0}{a_2}f, \qquad (3.34)
\end{aligned}
$$

where $f = 3$ for a broad topographic feature and $f = pw_2$ for a narrow topographic feature. Note that in the limit of weak coupling (i.e., $\kappa_{1,2} \to 0$) and weak topography (i.e., $D_0 \to 0$) these equations collapse to (2.10) and (2.11). Thus this Hamiltonian approach allows us to go beyond the asymptotic theory of section 3d.

4. Numerical simulations of the coupled KdV system

In this section we will examine the dynamics of the system of the full coupled KdV equations (2.5) numerically. We will set the frictional term $E = 0$, unless otherwise specified, and assume the form (3.7) for the topography. To integrate this system a semi-implicit pseudospectral code is used, in which the linear terms are treated using a Crank–Nicholson scheme and the nonlinear terms using an explicit leapfrog scheme. Periodic boundary conditions are imposed in the x direction. To avoid self-interaction of the fields due to radiation tunneling through the periodic boundaries, we introduce an artificial viscosity acting only near the boundaries. In the following we will simulate the behavior of the coupled KdV system with different parameter values and investigate the stability properties of the background and of possible coherent structures, that is, the steady-state solutions, and their interaction with topography. We recall that (A.15) determines the parameters while (2.8) and (3.23) determine the stability properties of the background and solitary-wave solution, respectively.

The basic dynamics of the coupling terms and the topographic forcing term are similar. The impact of an upper-layer solitary-wave disturbance or a topographic

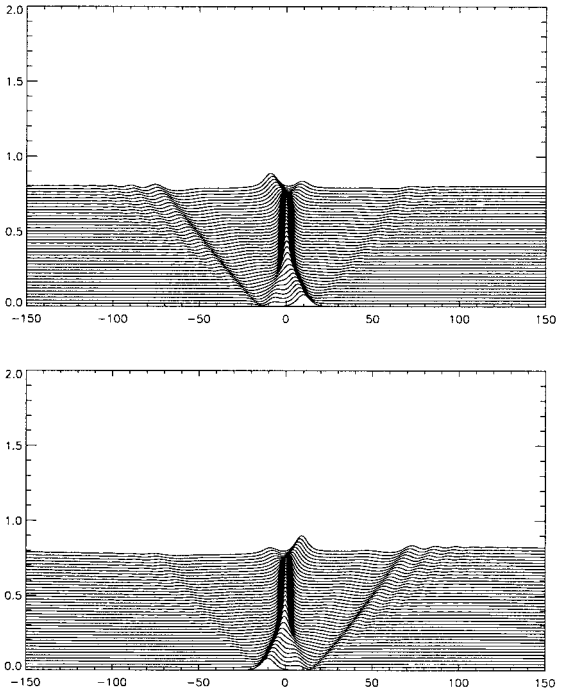

FIG. 5. Interaction of two solitary waves, where $\kappa_1 = -1.0$, $\kappa_2 = 1.0$, $\mu = -1$, $\lambda = -1$, $\Delta_1 = -1.5$, $\Delta_2 = 1.5$, $a_1 = a_2 = 0.08$, $D_0 = -0.1$, and $p = 122.0$.

feature on an undisturbed lower layer in a stable environment is to give birth to a secondary wave. Thus, if we suppose $A_2 = 0$ at $t = 0$, it follows from (2.5) that the further dynamics of the lower layer is given by $A_2 \approx \kappa_2 A_{1x} t$ or $A_2 \approx D_x t$, which has a dipole structure in both cases. The basic dynamics of solitary-wave interaction is determined by the interplay of these induced changes in amplitudes and the associated changes in wave speed according to (3.4).

Meteorological observations suggest that topography is not necessary for the creation and development of blocking systems but may enhance and amplify them (Egger et al. 1986). Having this in mind, we show that the effect of a topographic feature on the steady-state solutions of the unforced coupled KdV equations, as discussed in GG and therein associated with atmospheric blocking systems, is twofold: it may enforce the local character of blocking systems due to capturing traveling waves, and it may also enhance their amplitudes. As can be seen from Fig. 1 the amplifying influence of topography on the amplitude is largest for small Δ, that is, for small nontopographic steady-state solutions. This already indicates that, as Egger et al. (1986) suggest, topography may provide the forcing that leads to blocking systems that otherwise had amplitudes too small to be classified as mature blocking systems.

In Fig. 5 we show an interaction of two solitary waves meeting over a topographic feature with $D_0 = -0.1$ and $p = 122.0$ located at $x = 0$. For $D_0 = 0$ a similar picture is obtained, and the dynamics in both cases reflects the

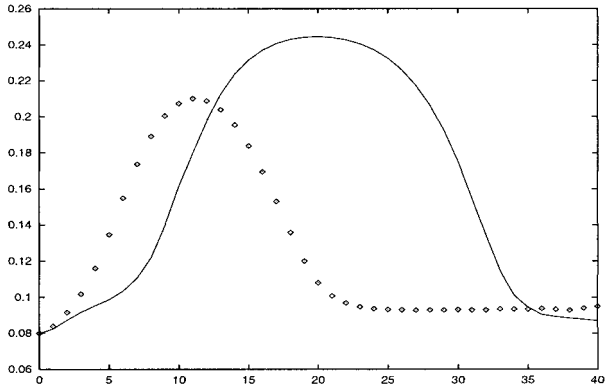

FIG. 6. Amplitudes a_1 as a function of time for the simulation depicted in Fig. 5. The dots represent the case $D_0 = 0$, the continuous line $D_0 = -0.1$.

quasi-blocked state of a saddle point discussed for the nontopographic case in GG. A comparison of the amplitudes for the upper layer of the topographic and nontopographic case is shown in Fig. 6. Due to symmetry the picture for the lower layer is similar. It shows that not only are the amplitudes larger, but also the transient quasi-blocked period is much longer. We note that topography may also trigger baroclinic instability if the forcing is large enough. An example for this is given in Fig. 7. The reason for this is simply that the change in amplitude of the solitary wave caused by topography may push the solitary wave into the unstable band of baroclinic instability as discussed in section 2 for $\kappa_1 \kappa_2$

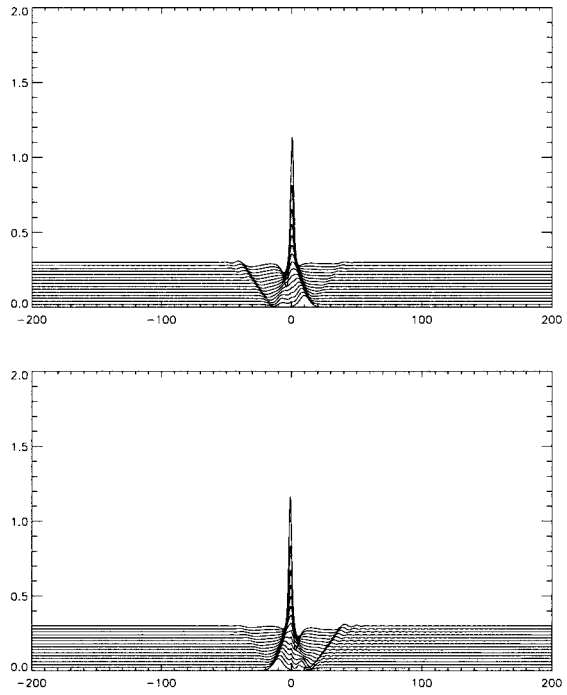

FIG. 7. Topographic forcing as a trigger to baroclinic instability. Parameters as in Fig. 5 but $D_0 = 0.168$ and $p = 0.2$.

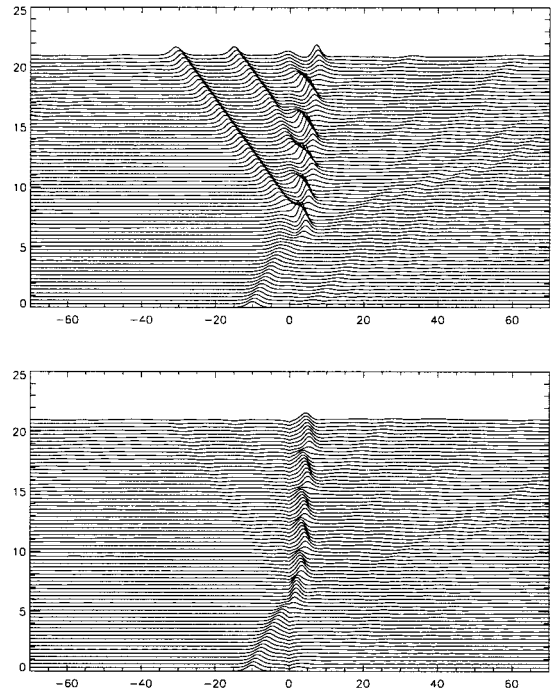

FIG. 8. Interaction of a stable center with topography, where $\kappa_1 = -0.7$, $\kappa_2 = -0.3$, $\mu = 1$, $\lambda = 1$, $\Delta_1 = 1.296$, $\Delta_2 = 1.696$, $a_1 = a_2 = 0.498$, $D_0 = -1.05$, and $p = 0.2$.

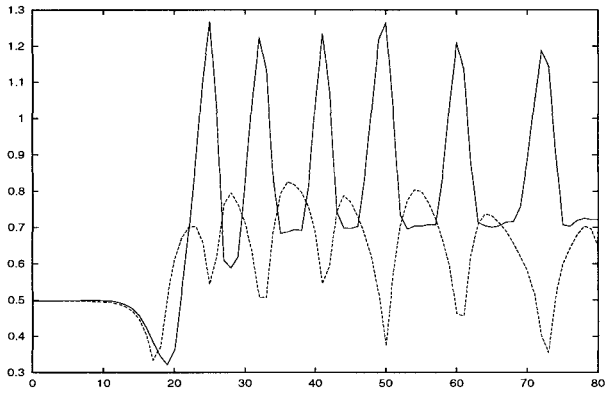

FIG. 9. Amplitudes $a_{1,2}$ as a function of time for the simulation depicted in Fig. 8. The continuous lines represent the upper layer a_1, the dotted line the lower layer a_2.

< 0. An examination for the interaction of a stable center with topography is given in Fig. 8. The amplitude of the upper- and lower-layer solitary waves are depicted in Fig. 9. The parameters are chosen such that the solitary waves represent a stable center in a nontopographic environment. The topography traps the traveling wave and leads to a well-localized coherent structure. Moreover, as can be seen from Fig. 9, the amplitudes rise significantly. We note that the duration of the larger-amplitude states are about 10 days if we assume a typical horizontal length scale of 1000 km, a typical velocity of the mean flow of 10 m s^{-1} and set the smallness parameter of the long-wave theory as $\delta = 0.1$. We also observe significant upstream waves, reminiscent of the single-layer forced KdV equation. Again for the case $\kappa_1\kappa_2 < 0$ baroclinic instability can be triggered. It is pertinent to mention that the parameter values chosen to obtain Fig. 8 do not support a topographic equilibrium solution, as can be readily seen from (3.12). This means that the locked state observed here is not a perturbed topographic steady-state solution but the result of an interaction of topography with a nontopographic stable steady-state solution.

The rise in the amplitude in both cases, for the center as well as for the saddle point, is due to the simple fact that topography enters Eq. (2.5) as a forcing term. The capture owes its existence to the stabilizing effect of topography under the condition $\kappa_1\mu < 0$ and $D_0 < 0$. We emphasize that topography does not change the character of the solutions but only adds new features to the types of solutions found in GG, that is, either characterized as stable centers or saddle points.

5. Discussion and summary

In this paper we have developed a weakly nonlinear, long-wave approximation for a topographically forced quasigeostrophic two-layer system with bottom Ekman damping. The dynamics of two interacting waves was found to be described by a pair of coupled Korteweg–de Vries equations. It has been our purpose to relate the solitary-wave solutions supported by this KdV system to coherent structures in the atmosphere, in particular to atmospheric blocking. The main focus was to investigate the influence of topography on solitary waves and the relevance of topographic forcing as a mechanism for the formation and development of blocking systems.

The validity of our theory as a model for atmospheric blocking has to be tested in two different ways. First, we have to show that the pair of coupled KdV equations does describe the dynamics of the quasigeostrophic system in the long-wave limit correctly, and is an appropriate approximation. Second, the results of our asymptotic theory have to be consistent with observational data.

We will start with the former, and we do so by looking at the time evolution of a solitary-wave steady-state solution of the coupled KdV equation (2.5) in the full quasigeostrophic two-layer system (2.1). The numerical scheme to integrate the quasigeostrophic two-layer system used here is the same as in GG, namely, a finite-difference code introduced by Holland (1978). Outgoing waves have been taken care of by using a sponge layer in which all time derivatives artificially are set equal to zero near the boundary and then are smoothly connected to the exact value in the interior. The mean flow is supposed to be of the form $U_i = U_{i0}(y - l_i)^2 \sin[\pi/L(y - y_{\max})]$, where L is the channel width and U_{i0}, l_i are free parameters. In Fig. 10 we show an example of a stable steady-state solution. For the mean flow we chose

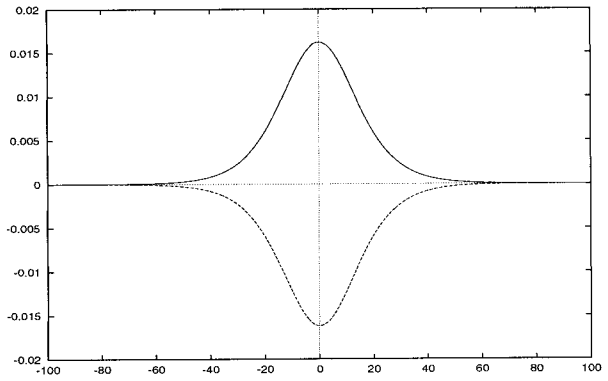

FIG. 10. Steady-state solution representing a topographically forced center after $T = 400$. The continuous line refers to the upper layer, the dotted line to the lower layer.

$U_{10} = 0.049$, $U_{20} = 0.055$, $L = 2$,$y_{\max} = 1$, $l_1 = 9$, and $l_2 = -9$, and we set $\beta = 0.0025$, $F_1 = 0.005$, $F_2 = 0.006\,25$, $D_0 = -0.16$, $p = 0.05$, and $\delta^2 = 0.1$. The corresponding parameters for the KdV equations are calculated using (A.15) and the scaling described in the appendix to $a_1^* = -0.12$, $a_2^* = 0.12$, $\lambda = 0.9$, $\mu = -0.9$, $\Delta_1 = 0.11$, $\Delta_2 = 0.12$, $\kappa_1 = 0.1$, and $\kappa_2 = 0.1$, and we obtain for the time stretching $t = 60T$. In the x direction we used 900 grid points, in the y direction 20. The solitary wave is clearly stable in the quasigeostrophic system as well as in the KdV system.

To confirm our theory that the coupled Korteweg–de Vries system is indeed a good approximation for the quasigeostrophic two-layer system in the weakly nonlinear, long-wave limit, we will also show a simulation for a set of parameters that does not yield a steady state but instead shows solitary-wave interaction. Fig. 11 shows the two solitary waves after a time $T = 200$. The corresponding snapshot of the two solitary waves in the KdV system is depicted in Fig. 12. The mutual interaction in both cases are the same.

The numerics and Figs. 10–12 show that the solitary waves obtained as approximate solutions in the asymptotic theory do survive in the full quasigeostrophic two-layer system and we can claim that the coupled KdV equations (2.5) are indeed a valid approximation for the quasigeostrophic system (2.1) in the weakly nonlinear, long-wave approximation and do represent the dynamics in this limit.

We do not attempt to make accurate quantitative comparisons of our asymptotic theory and the observational data or numerical simulations of real atmospheric flows as our solitary-wave model is designed basically to extract possible scenarios and mechanisms. Moreover, it seems more appropriate to do a quantitative comparison of observational data and a set of numerical simulations of the full quasigeostrophic two-layer system. This aspect is currently under investigation and will be reported in detail elsewhere. Nevertheless, we can draw qualitative conclusions and show consistency of our model with the data.

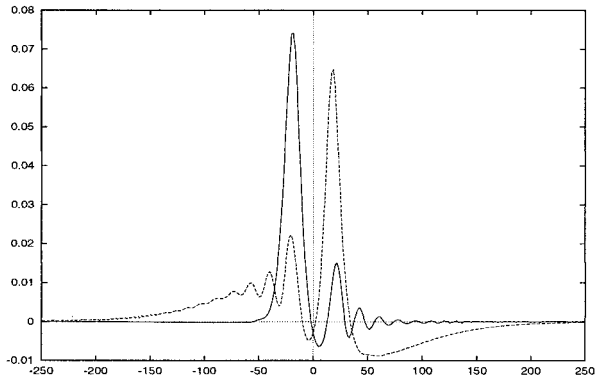

FIG. 11. Interaction of two topographically forced solitary waves in the quasigeostrophic two-layer system at $T = 200$, which were initially both centered around the topography at $x = 0.0$. The continuous line refers to the upper layer, the dotted line to the lower layer. The parameters chosen are $U_{10} = -0.05$, $U_{20} = 0.06$, $L = 2$, $y_{\max} = 1$, $l_1 = 9$, $l_2 = 8$, $\beta = 0.000\,15$, $F_1 = 0.015$, $F_2 = 0.015$, $D_0 = -0.16$, $p = 30.0$, and $\delta^2 = 0.15$. In the x direction we used 600 grid points, in the y direction 10.

We will briefly discuss the magnitude of the parameters of the system of coupled KdV equations (2.5). Since the parameters reflect the details of the mean flow structures, we need to use observational data, especially for the meridional gradients in both layers. We will estimate the order of the magnitude using a rough but reasonable approximation. We put $U_1 = \gamma U_2$, where $\gamma = D_2/D_1$ so that each layer has the same mass flux. This rough approximation yields

$$\mu \approx \gamma, \qquad \lambda \approx \gamma, \qquad \kappa_1 \approx F_1, \qquad \kappa_2 \approx \gamma\sigma_2 F_2.$$

If we choose $D_2 = 10$ km as the height of the tropopause and $D_1 = 2.5$ km as the height of the tropopause with densities $\rho_1 = 0.45$ kg m^{-3} and $\rho_2 = 0.85$ kg m^{-3}, and

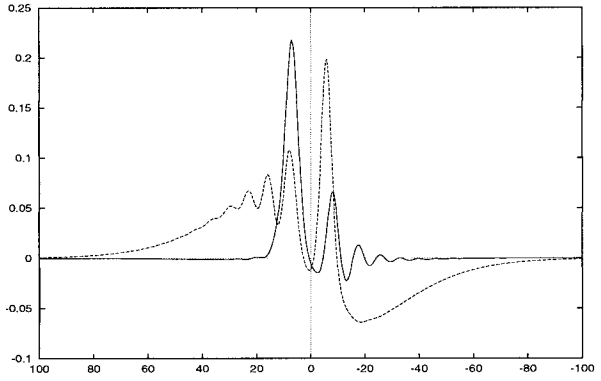

FIG. 12. Interaction of two topographically forced solitary waves in the KdV system at time $t = 15$ corresponding to Fig. 11. The continuous line refers to the upper layer, the dotted line to the lower layer. The corresponding parameters for the KdV equations of the parameters given in Fig. 11 yield for the KdV equation $a_1 = 0.23$, $a_2 = 0.20$, $\lambda = -1.06$, $\mu = -0.94$, $\Delta_1 = 0.10$, $\Delta_2 = -0.11$, $\kappa_1 = 0.10$, $\kappa_2 = -0.11$, $D_0 = -0.16$, and $p = 30.0$, and we obtain for the time stretching $t = 14T$. Since $\lambda_2 < 0$ we had to let $x \to -x$ to compare it with Fig. 11.

recall the typical synoptic scales as $L = 1000$ km, $U_0 = 10$ m s^{-1}, and $f_0 = 10^{-4}$ s^{-1}, and take the smallness parameter $\delta = 0.5$, we obtain $\mu \approx \lambda \approx 4$, $\kappa_1 \approx 0.1$, and $\kappa_2 \approx 0.2$. Thus, realistic flow structures imply a weak coupling situation, which we used in our perturbation theory. Values for the height of the topography D_0, which range from 0.1 to 1.0, correspond to topographical features of 500 m to 5 km.

The results from the asymptotic theory and the numerical simulation of the KdV equations support the observations of Egger et al. (1986) that topography is not essential for the formation and maintenance of blocking systems but may provide preferred conditions under which blocking systems can occur and develop. Our theory is consistent with this observation since topography does not introduce fundamentally new solutions compared to the nontopographic case previously discussed in GG, but supports features highly supportive for atmospheric blocking. Of the various phenomena investigated here the most significant from a meteorological point of view are wave capturing, direct resonant forcing, and multiple equilibria. We will briefly summarize these features and their relevance to blocking systems.

Topographic forcing was shown to modify steady-state solutions of the nontopographic case and their interaction either by direct resonant forcing or by capturing traveling waves. In particular, we have shown that quasi-locked states exhibit longer blocking periods and larger amplitude states than they had in the nontopographic case. Furthermore, stable waves (i.e., centers in the phase-plane analogy) moving toward a topographic feature may be captured and stay locked to it. Again the resulting steady-state solution shows larger amplitudes than in the nontopographic case. We have also demonstrated that topography can trigger baroclinic instability in incident waves.

In GG we found multiple quasi equilibria of saddle points where small perturbations of incident waves would either lead to a repulsion regime or a quasi-locked state, the latter being highly suggestive of transient blocking systems. Besides these nontopographic multiple equilibria we have found here multiple equilibria whose nature is solely due to topographical forcing. We found two kinds of topographical multiple equilibria; either as different amplitude states where energy conversion due to baroclinic processes is balanced by topographical forcing, or when small Ekman damping is included and we assume a balance between topographical forcing and frictional dissipation, states of different location relative to the topography. The difference of the amplitudes of the topographic steady-state solution and the nontopographic steady-state solution is most significant for small amplitudes and can be neglected for large amplitudes. Hence, topography may provide the energy for high pressure fields to be actually regarded as a blocking highs (see Egger et al. 1986). Unlike the multiple equilibria found by Charney and DeVore (1979), the local multiple equilibria do not rely on the existence of a globally resonant Rossby wave.

Further research needs to be done on solitary-wave interactions in the full quasigeostrophic two-layer system, and is currently under investigation. Furthermore, since in the Southern Hemisphere topographic forcing is less significant than thermal forcing of sea surface temperature anomalies, we will report on this case in a sequel to this paper and present an asymptotic theory analogous to those used here.

Acknowledgments. We gratefully acknowledge the support of the Deutscher Akademischer Austauschdienst, which sponsored this work through the HSP III; of the CRC–Southern Hemisphere Meteorology; and the support from ARC Grant A89600523.

APPENDIX

Derivation of Coupled KdV Equations

We summarize here the derivation described in our previous paper GG. If we insert the boundary conditions (2.2) into the quasigeostrophic equations (2.1), the perturbations $\psi_{1,2}$ satisfy

$$\left(\frac{\partial}{\partial t} + U_n\frac{\partial}{\partial x}\right)q_n + \psi_{nx}Q_{ny} + J(\psi_n, q_n) = \begin{cases} 0 \\ -\dfrac{E_V^{1/2}}{2\epsilon}\Delta\psi_2, \end{cases} \tag{A1}$$

where $n = 1, 2$, respectively, and

$$q_1 = \nabla^2\psi_1 + F_1(\psi_2 - \sigma_1\psi_1), \tag{A2}$$

$$q_2 = \nabla^2\psi_2 + F_2(\psi_2 - \sigma_2\psi_1) + \eta_B, \tag{A3}$$

$$Q_{1y} = \beta - U_{1yy} - F_1(U_2 - \sigma_1 U_1), \tag{A4}$$

$$Q_{2y} = \beta - U_{2yy} + F_2(U_2 - \sigma_2 U_1), \tag{A5}$$

with the Jacobian defined by

$$J(a, b) = a_x b_y - a_y b_x.$$

The boundary conditions transform into

$$\psi_{1,2} = \text{const} \quad \text{at } y = -L, 0. \tag{A6}$$

Note that we adopt the usual convention that the frictional term in (A1) acts only on the perturbation field; that is, an appropriate forcing term is added to the right-hand side of (2.1) to maintain the mean current.

For the weakly nonlinear long-wave analysis we introduce the following scales:

$$X = \delta x$$

$$T = \delta^3 t$$

$$\psi_i = \delta^2\psi_i^{(0)} + \delta^4\psi_i^{(1)} + \cdots$$

$$U_i = U_i^{(0)} + \delta^2 U_i^{(1)} + \cdots,$$

where δ is a small parameter, the inverse of which mea-

sures the horizontal scale of the disturbance. Next, we rescale the Froude numbers

$$F_i \to \delta^2 F_i. \tag{A7}$$

It follows that our model is valid for situations where the internal Rossby radius of deformation is of the order of the long horizontal scale. Further, we scale

$$\beta \to \delta^2 \beta$$

$$\eta_B \to \delta^4 \eta_B$$

$$\frac{E_V^{1/2}}{2\epsilon} \to \delta^3 E$$

so that $Q_{iy} \approx -U_{iyy}$ at the lowest order. This scaling of the bottom friction means that the timescale for frictional damping is measured by the slow time T. Of course, from the point of view of applications, the scaling is given by the topography and the thereby-introduced spatial scale. The remaining scaling then follows from the condition of the waves being in resonance with the topography and the conditions described above for the potential vorticity gradient. Substituting this scaling into Eq. (A1), we obtain to the lowest order $O(\delta^3)$

$$U_i^{(0)} \psi_{iXyy}^{(0)} - U_{iyy}^{(0)} \psi_{iX}^{(0)} = 0,$$

from which we conclude that

$$\psi_i^{(0)}(X, T, y) = A_i(X, T) U_i^{(0)}(y). \tag{A8}$$

Hence, the meridional structure of ψ_i is entirely determined by the mean currents at the leading order.

The $O(\delta^5)$ terms give us two evolution equations for the amplitudes A_i for each layer. We reiterate that the reason for the occurrence of two coupled equations is the scaling of the Froude numbers (A7), which implies the existence of two independent modes at leading order. We obtain

$$U_i^{(0)} \psi_{iXyy}^{(1)} - U_{iyy}^{(0)} \psi_{iX}^{(1)} + G_i = 0, \tag{A9}$$

where

$$\begin{aligned} G_1 = {} & A_{1T} U_{1yy}^{(0)} + U_1^{(0)} A_{1XXX} U_1^{(0)} \\ & + F_1 U_1^{(0)} (U_2^{(0)} A_{2X} - \sigma_1 U_1^{(0)} A_{1X}) + U_1^{(1)} A_{1X} U_{1yy}^{(0)} \\ & + A_{1X} U_1^{(0)} [\beta - U_{1yy}^{(1)} - F_1 (U_2^{(0)} - \sigma_1 U_1^{(0)})] \\ & + A_1 A_{1X} (U_1^{(0)} U_{1yyy}^{(0)} - U_{1y}^{(0)} U_{1yy}^{(0)}), \end{aligned} \tag{A10}$$

$$\begin{aligned} G_2 = {} & A_{2T} U_{2yy}^{(0)} + U_2^{(0)} A_{2XXX} U_2^{(0)} \\ & - F_2 U_2^{(0)} (U_2^{(0)} A_{2X} - \sigma_2 U_1^{(0)} A_{1X}) + U_2^{(1)} A_{2X} U_{2yy}^{(0)} \\ & + A_{2X} U_2^{(0)} [\beta - U_{2yy}^{(1)} + F_2 (U_2^{(0)} - \sigma_2 U_1^{(0)})] \\ & + A_2 A_{2X} (U_2^{(0)} U_{2yyy}^{(0)} - U_{2y}^{(0)} U_{2yy}^{(0)}) + \gamma U_2^{(0)} \eta_{BX} \\ & + E A_2 U_{2yy}^{(0)}. \end{aligned} \tag{A11}$$

The solvability conditions are obtained by integrating (A9) with respect to y, so that, on using the boundary conditions (A6), we get

$$\int_{-L}^{0} G_i \, dy = 0. \tag{A12}$$

On substituting the expressions (A10) and (A11) for G_i we obtain the amplitude equations for A_i:

$$A_{1T} + \Delta_1 A_{1X} - \mu_1 A_1 A_{1X} - \lambda_1 A_{1XXX} - \kappa_1 A_{2X} = 0, \tag{A13}$$

$$A_{2T} + \Delta_2 A_{2X} - \mu_2 A_2 A_{2X} - \lambda_2 A_{2XXX} - \kappa_2 A_{1X} = D_X - E A_2, \tag{A14}$$

where

$$\begin{aligned} I_n &= -[U_{ny}^{(0)}]_{-L}^{0}, \\ I_n \lambda_n &= \int_{-L}^{0} U_n^{(0)^2} \, dy, \\ I_n \mu_n &= -[U_{ny}^{(0)^2}]_{-L}^{0}, \\ I_1 \Delta_1 &= -\int_{-L}^{0} (\beta - F_1 U_2^{(0)}) U_1^{(0)} \, dy - [U_1^{(1)} U_{1y}^{(0)}]_{-L}^{0}, \\ I_2 \Delta_2 &= -\int_{-L}^{0} (\beta - \sigma_2 F_2 U_1^{(0)}) U_2^{(0)} \, dy - [U_2^{(1)} U_{2y}^{(0)}]_{-L}^{0}, \\ I_1 \kappa_1 &= F_1 \int_{-L}^{0} U_1^{(0)} U_2^{(0)} \, dy, \\ I_2 \kappa_2 &= \sigma_2 F_2 \int_{-L}^{0} U_1^{(0)} U_2^{(0)} \, dy, \\ I_2 D &= \eta_B \int_{-L}^{0} U_2^{(0)} \, dy. \end{aligned} \tag{A15}$$

Equations (A13) and (A14) have the form of two coupled KdV equations and, as expected, are similar to those derived by Mitsudera (1994). Note that for meridional symmetric and antisymmetric flows, or more generally just for $U_{iy}^{(0)} = 0$ at the boundaries, the nonlinear term vanishes. The coefficients μ_i determine the polarity of the solitary waves. Before proceeding further, we shall rescale Eqs. (A13) and (A14) for convenience. We put

$$T \to \frac{T}{|\lambda_2|}, \qquad X \to (\mathrm{sign}\lambda_2) X, \qquad A_n \to \frac{6\lambda_2}{\mu_2} A_n,$$

$$\Delta_n \to \lambda_2 \Delta_n, \qquad \kappa_n \to \lambda_2 \kappa_n, \qquad \mathcal{F} \to |\lambda_2| \mathcal{F},$$

$$D \to \lambda_2 D,$$

and

$$\mu = \frac{\mu_1}{\mu_2}, \qquad \lambda = \frac{\lambda_1}{\lambda_2},$$

in order to get

$$A_{1T} + \Delta_1 A_{1X} - 6\mu A_1 A_{1X} - \lambda A_{1XXX} - \kappa_1 A_{2X} = 0,$$
$$A_{2T} + \Delta_2 A_{2X} - 6A_2 A_{2X} - A_{2XXX} - \kappa_2 A_{1X} = D_X - EA_2. \quad \text{(A16)}$$

REFERENCES

Cehelsky, P., and K. K. Tung, 1985: Theories of multiple equilibria and weather regimes—A critical reexamination. Part II: Baroclinic two-layer models. *J. Atmos. Sci.,* **42,** 2804–2819.

Charney, J., and J. DeVore, 1979: Multiple flow equilibria in the atmosphere and blocking. *J. Atmos. Sci.,* **36,** 1205–1216.

Christensen, C. W., and A. Wiin-Nielsen, 1996: Blocking as a wave–wave interaction. *Tellus,* **48,** 254–271.

Davey, M. K., 1981: A quasi-linear theory for rotating flow over topography. Part II: Beta plane annulus. *J. Fluid Mech.,* **103,** 297–320.

Dickinson, R. E., 1978: Rossby waves. Long-period oscillations of oceans and atmospheres. *Annu. Rev. Fluid Mech.,* **10,** 159–195.

Egger, J., W. Metz, and G. Mueller, 1986: Forcing of planetary-scale blocking anticyclones by synoptic-scale eddies. *Advances in Geophysics,* Vol. 29, Academic Press, 183–197.

Fandry, C. B., and L. M. Leslie, 1984: A two-layer quasi-geostrophic model of summer trough formation in the Australian subtropical easterlies. *J. Atmos. Sci.,* **41,** 807–818.

Gottwald, G. A., and R. H. J. Grimshaw, 1999: The formation of coherent structures in the context of blocking. *J. Atmos. Sci.,* **56,** 3640–3662.

Grimshaw, R., and H. Mitsudera, 1993: Slowly varying solitary wave solutions of the perturbed Korteweg–de Vries equation revisited. *Stud. Appl. Math.,* **90,** 75–86.

——, E. Pelinovsky, and X. Tian, 1995: Interaction of a solitary wave with an external force. *Physica,* **D77,** 405–433.

Hansen, A. R., and A. Sutera, 1984: A comparison of the spectral energy and enstrophy budgets of blocking versus non-blocking periods. *Tellus,* **36,** 52–63.

Helfrich, K. R., and J. Pedlosky, 1993: Time-dependent isolated anomalies in zonal flows. *J. Fluid Mech.,* **251,** 377–409.

——, and ——, 1995: Large-amplitude coherent anomalies in baroclinic zonal flows. *J. Atmos. Sci.,* **52,** 1615–1629.

Holland, W. R., 1978: The role of mesoscale eddies in the general circulation of the ocean—Numerical experiments using a wind-driven quasigeostrophic model. *J. Phys. Oceanogr.,* **8,** 363–392.

Illari, L., 1984. A diagnostic study of the potential vorticity in a warm blocking anticyclone. *J. Atmos. Sci.,* **41,** 3518–3526.

Johnson, R., 1973: On an asymptotic solution of the Korteweg–de Vries equation with slowly varying coefficients. *J. Fluid Mech.,* **86,** 415–446.

Kalnay, E., and K. C. Mo, 1986: Mechanistic experiments to determine the origin of short-scale Southern Hemisphere stationary Rossby waves. *Advances in Geophysics,* Vol. 29, Academic Press, 415–442.

Karpman, V., and E. Maslov, 1978: Structure of tails produced under the action of perturbations on solitons. *Sov. Phys. JETP,* **48,** 252–259.

Kaup, D., and A. Newell, 1978: Solitons as particles, oscillators, and in slowly changing media: A singular perturbation theory. *Proc. Roy. Soc. London,* **361A,** 412–446.

Legras, B., and M. Ghil, 1985: Persistent anomalies, blocking and variation in atmospheric predictability. *J. Atmos. Sci.,* **42,** 433–471.

Lindzen, R. S., 1986: Stationary planetary waves, blocking, and interannual variability. *Advances in Geophysics,* Vol. 29, Academic Press, 251–276.

Lupo, A., and P. Smith, 1995: Planetary and synoptic-scale interactions during the life cycle of a midlatitude blocking anticyclone over the North Atlantic. *Tellus,* **47A,** 575–596.

Malanotte-Rizzoli, P., and P. Malguzzi, 1987: Coherent structures in a baroclinic atmosphere. Part III: Block formation and eddy forcing. *J. Atmos. Sci.,* **44,** 2493–2505.

Malguzzi, P., and P. Malanotte-Rizzoli, 1984: Nonlinear stationary Rossby waves on nonuniform zonal winds and atmospheric blocking. Part I: The analytical theory. *J. Atmos. Sci.,* **41,** 2620–2628.

——, and ——, 1985: Coherent structures in a baroclinic atmosphere. Part II: A truncated model approach. *J. Atmos. Sci.,* **42,** 2463–2477.

Mitsudera, H., 1994: Eady solitary waves: A theory of type B cyclogenesis. *J. Atmos. Sci.,* **51,** 3137–3154.

——, and R. Grimshaw, 1991: Generation of mesoscale variability by resonant interaction between a baroclinic current and localized topography. *J. Phys. Oceanogr.,* **21,** 737–765.

——, and ——, 1994: Capture and resonant forcing of solitary waves by the interaction of a baroclinic current with topography. *J. Phys. Oceanogr.,* **24,** 2217–2244.

Mullen, S. L., 1987: Transient eddy forcing and blocking flows. *J. Atmos. Sci.,* **44,** 3–22.

Patoine, A., and T. Warn, 1982: The interaction of long, quasi-stationary baroclinic waves with topography. *J. Atmos. Sci.,* **39,** 1018–1025.

Pedlosky, J., 1987: *Geophysical Fluid Dynamics.* 2d ed. Springer-Verlag, 710 pp.

Shutts, G. J., 1983: The propagation of eddies in effluent jet streams: Eddy vorticity forcing of 'blocking' flow fields. *Quart. J. Roy. Meteor. Soc.,* **109,** 737–761.

——, 1986: A case study of eddy forcing during an Atlantic blocking episode. *Advances in Geophysics,* Vol. 29, Academic Press, 135–162.

Tung, K. K., and A. J. Rosenthal, 1985: Theories of multiple equilibria—A critical reexamination. Part I: Barotropic models. *J. Atmos. Sci.,* **42,** 2804–2819.

Warn, T., and B. Brasnett, 1983: The amplification and capture of atmospheric solitons by topography: A theory of onset of regional blocking. *J. Atmos. Sci.,* **40,** 28–40.

Yano, J., and H. Mukougawa, 1992: The attractor dimension of a quasi-geostrophic two layer system. *Geophys. Astrophys. Fluid Dyn.,* **65,** 77–91.